Growth of single crystals in material research

Author: Anežka Bendová[1]

Supervisor: Jiří Pospíšil[1]

[1]*Charles University, Faculty of Mathematics and Physics, Department of Condensed Matter Physics, Ke Karlovu 5, 12116 Prague 2, Czech Republic*

Abstract

The subject of this work was an optimization of the single crystal growth of various materials. Various single crystal growth methods such as Flux, Bridgman, Czochralski, Floating zone and Chemical vapour transport were tested on materials of various classes. The most stressed materials are heavy fermion semiconductors $U_3T_3X_4$ where T is a transition metal T = Ni, Pd and Pt and X = Sb or Bi as well as Ce_3Al_{11}. Other materials discussed in this work are semimetallic material U_2Ru_2Sn, ferromagnetic superconductor UCoGe doped with Ir, various Sapphire based materials, antifferromagnetic and possible semimetallic material UNiSn and at last known van der Waals ferromagnet VI_3. The properties and parameters of various techniques were tested and optimized for achieving the highest possible quality of single crystals.

Keywords

Single crystal, Flux, Bridgman method, Czochralski method, Floating Zone method

Introduction

Naturally, single crystals have higher purity and less defects than the common polycrystalline materials. Exclusive property connected with single crystals is anisotropy, which means that physical properties depend on the crystallographic direction along which is measured or observed. The study of solid matter performed on single crystals is the only way to obtain the highest quality experimental data, valuable results, and complex ideas about the origin of specific material properties. The only obstacle is the growth of the single crystals. Sometimes it can be very difficult to grow a single crystal of specific materials. The single crystal growth methods can vary from very simple and cheap techniques to the complex expensive processes. To understand deeply the single crystal growth process is a complex assignment.

1 The usage of single crystals

The solid matter in the form of single crystals is important both in advance research but also applications. Fundamental research performed on single crystals provides more accurate data about material's intrinsic properties than polycrystalline matter where anisotropic properties are averaged creating the sample isotropic. Other important advantage of single crystal is less defects and no grain boundaries. Without defects and grain boundaries, the crystal gains more precise properties in mechanics, electronics and optics. Because of this, single crystals are commonly used in industrial segment. Single crystal materials usually occur in engines or generators such as turbine blades, semi-conductors, detectors (infrared or radiation sensors), optics and lasers [1]. Silicon is the most common material used for production of microchips and photovoltaic cells, which are used in computers, phones, cars and many other electronic devices.

2 Results and discussion

This chapter describes the instrumentation, which I have used for single crystal growth in MGML laboratories in DCMP and summarizes my achieved experimental results. All single crystals grown by specific methods are summarized in Table 1.

Single crystal growth method	Materials
Flux growth	$U_3T_3Sb_4$
	$U_3T_3Bi_4$
	Ce_3Al_{11}
	$CeCd_3P_3$
Bridgman method	$U_3Pt_3Sb_4$
Czochralski method	U_2Ru_2Sn
	$UCo_{0.95}Ir_{0.05}Ge$
Floating Zone method	Sapphire based materials
	UNiSn
Chemical vapour transport method	VI_3

Table 1: List of materials grown by different methods.

2.1 Flux growth

2.1.1 Description of method

Elements were weighted to a small alumina crucible. This crucible was put into the flat bottom quartz tube, and on the top I put identical alumina crucible upside-down filled with quartz wool. On top of the upper crucible further quartz wool was placed to protect the quartz ampoule against braking during the decanting process in a centrifuge.

Then, the tube was attached to a vacuum unit and evacuated down to vacuum limit 10^{-6} mbar (Fig. 1). To improve the vacuum by degas process, quartz ampoule was inserted to a movable furnace and heated up 300°C for several hours.

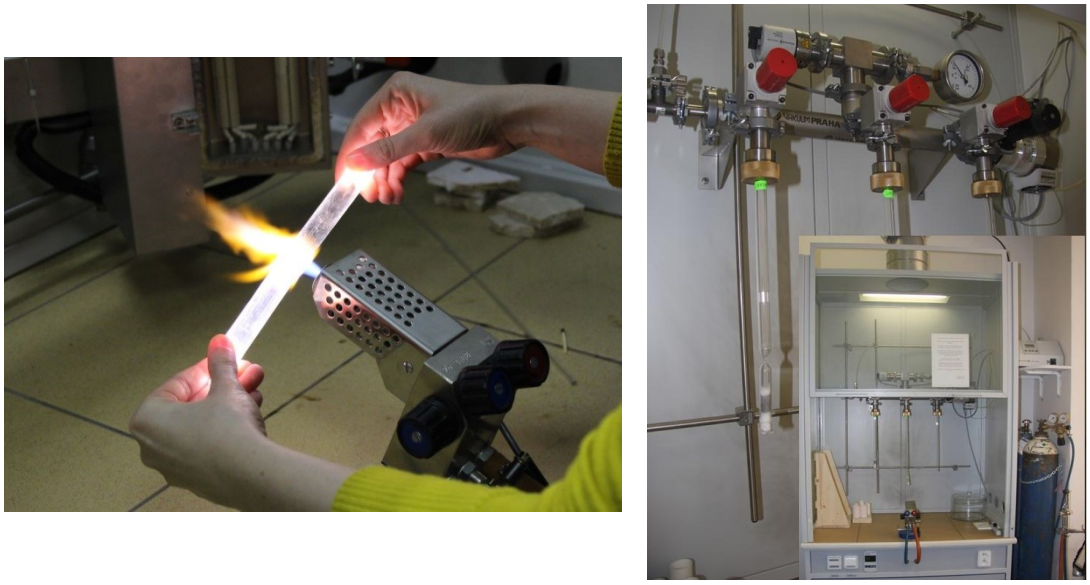

Figure 1: Making of the neck in quartz tube (left) and vacuum unit with glass sealing station (right) [2].

When the ampoule is sealed it is put in a bigger alumina crucible to keep it upright in the chamber of the furnace (Fig. 2). After the termination of the growth process in the furnace, the ampoule is put quickly upside-down into a centrifuge in order to separate excess of the solvent from the single crystals. The upper temperature and the cooling profiles vary for different materials.

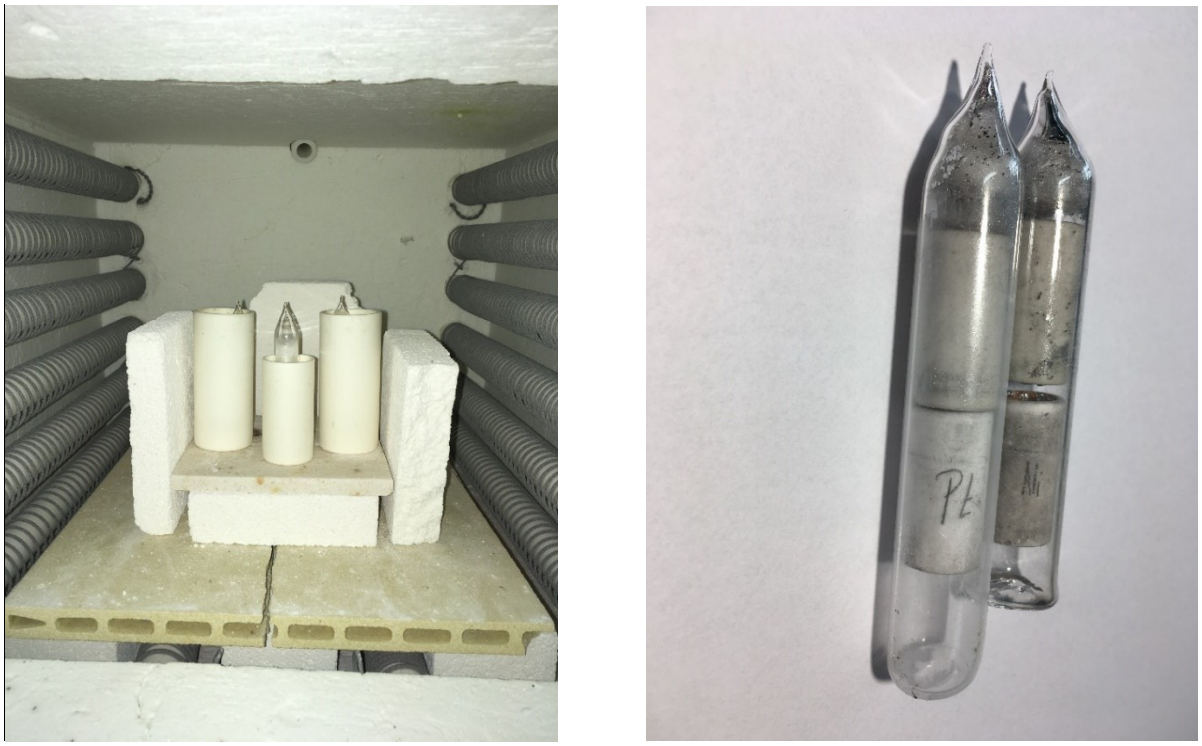

Figure 2: Furnace with ampoules in big alumina crucibles (left) and ampoules after decanting (right). The separated rest of the solvent element is visible in the upper tip of ampoules.

2.1.2 $U_3T_3Sb_4$ series

First materials grown were from an $U_3T_3Sb_4$ series where T is a transition metal T = Ni, Pd and Pt. These materials are expected to act as heavy fermion semiconductor with metal insulator transition [3]. I performed four attempts to grow these materials.

These compounds were grown from Sb self-flux [3]. The temperature profile is shown in Figure 3. The stoichiometric ratios of the elements were determined from the phase diagrams (Fig. 4). The atomic ratios for the growth were selected as shown in the picture. The solubility of Pt and U in Sb is similar. On the other hand, solubility of Pd and Ni is significantly higher in Sb than U.

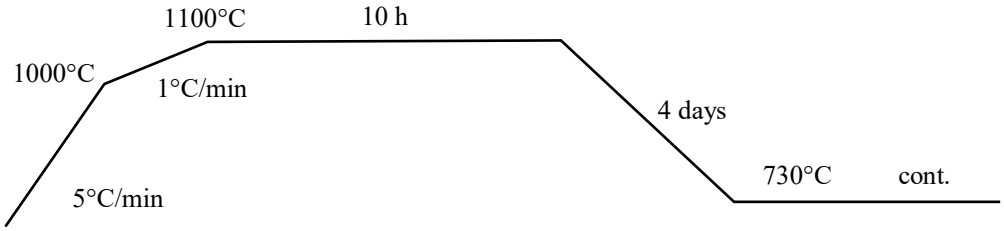

Figure 3: Temperature profile for the first series of $U_3T_3Sb_4$ material.

The obtained single crystals of different morphologies were obtained in U-Ni-Sb system (Fig. 5). The composition of the single crystals was found by microprobe analysis as U_3NiSb_5, which is an unreported new phase. Since the solubility of Ni in the Sb-flux is significantly higher than U process, it was repeated with two different ratios rich on Ni of 10:4:1 and 10:3:1 (Sb:Ni:U). Results of these repeated materials are in further text.

The obtained single crystals from the solution of U-Pd-Sb (Fig. 5) were in a shape of small plates. The composition of the single crystals was U_3PdSb_5 which is also an unreported new phase as Ni single crystals had. With Pd, there is also a problem with significantly higher solubility in Sb-flux than U; so I decided to repeat this material with ratio of 10:5:1 (Sb:Pd:U).

The obtained single crystals of U-Pt-Sb system (Fig. 5) were in the shape of polyhedrons. The single crystal's compositions came out as if there are two different compositions. One composition is USb_2, which is well-known antiferromagnet T_N = 203 K [5]. The other one was $PtSb_2$, which is also a well-known narrow-band semiconductor [6].

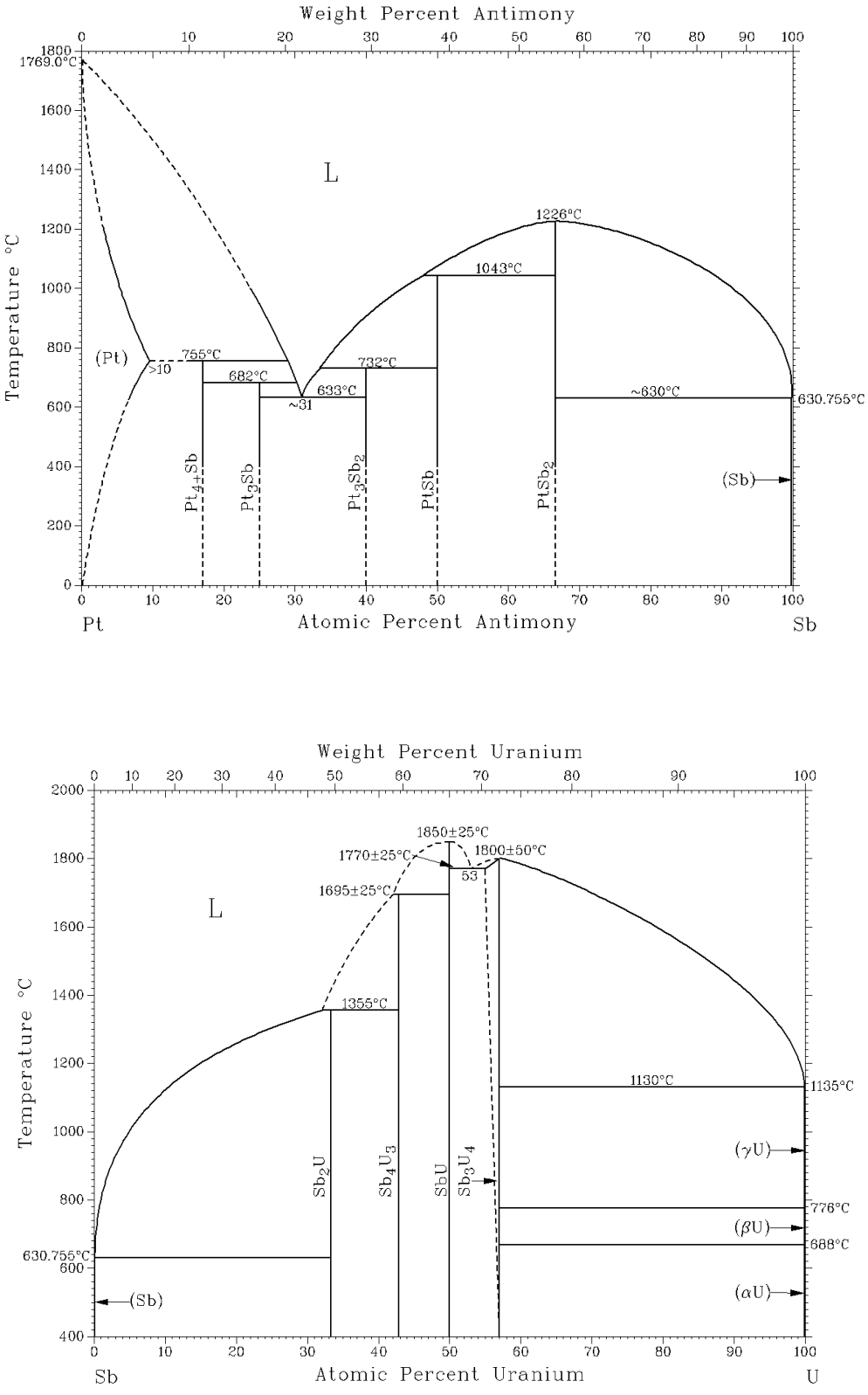

Figure 4: Phase diagrams of Pt – Sb and Sb – U in atomic percentage [4].

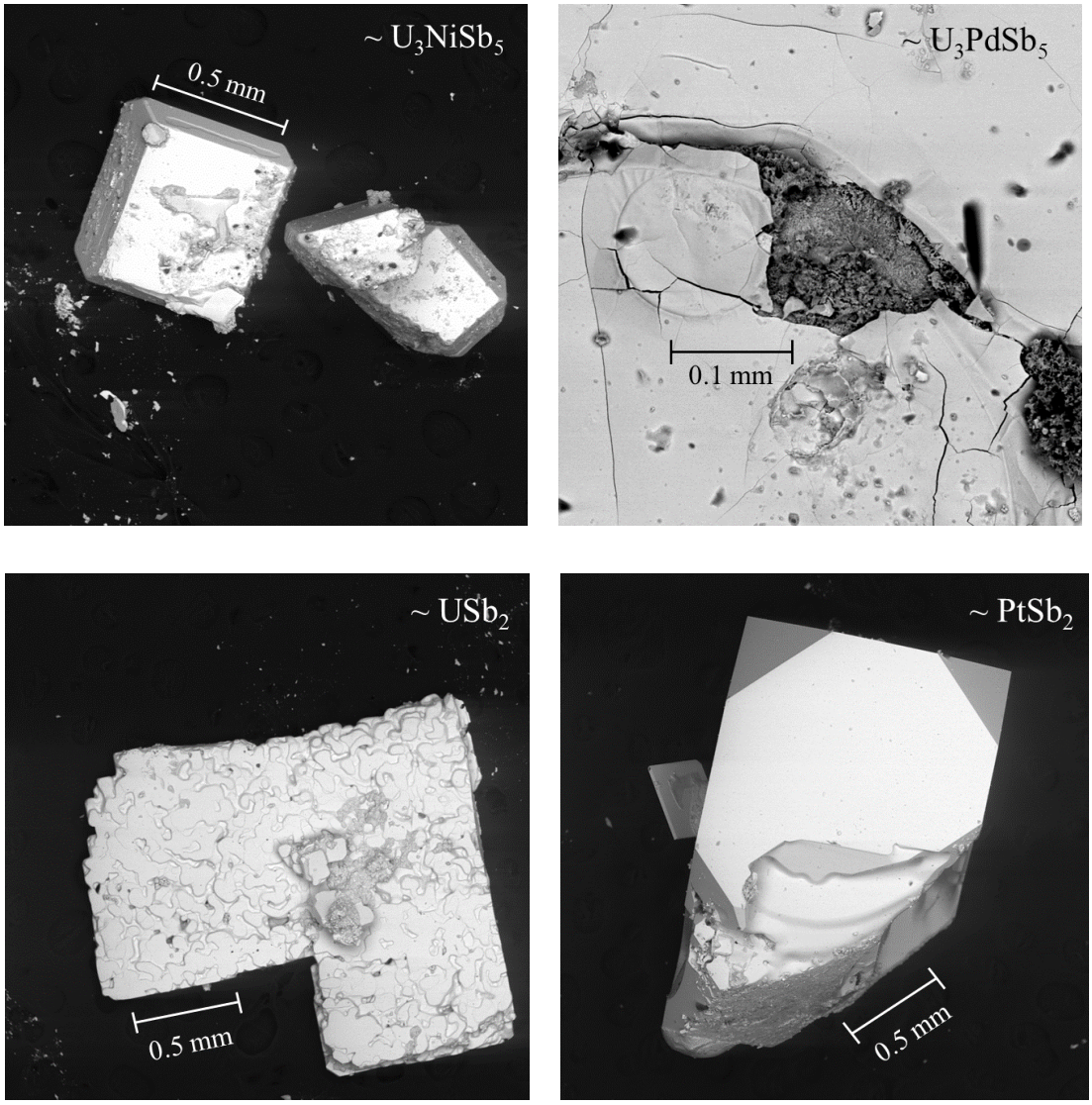

Figure 5: Single Crystals of the U-T-Sb system obtained from first series of material grown from Sb flux.

Because of small amount of single crystals in the first series of $U_3Ni_3Sb_4$ and $U_3Pd_3Sb_4$ due to high solubility of Pd and Ni in Sb, second series was prepared with higher concentration of Pd and Ni. Identical temperature profile was used (Fig. 3).

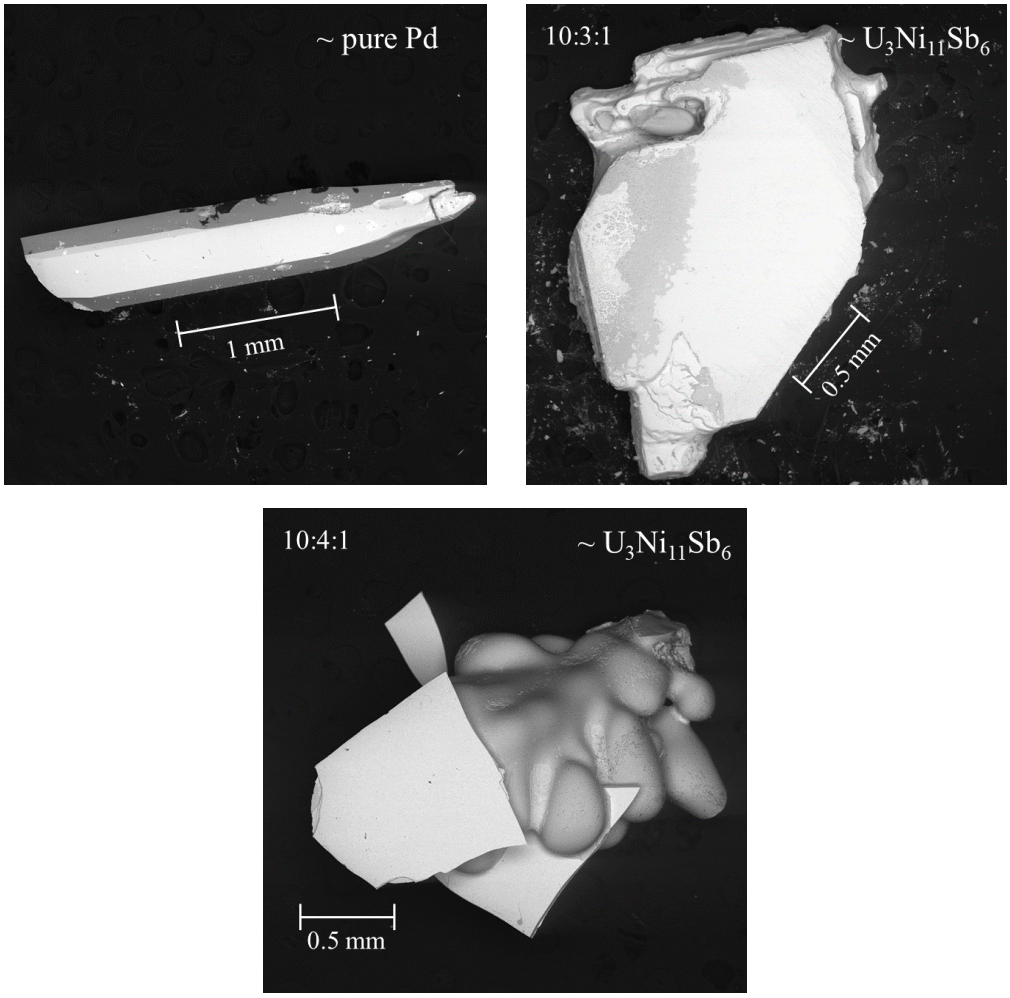

Figure 6: Single crystals of U-Ni-Sb and U-Pd-Sb systems obtained from second series of materials.

The obtained single crystals of U-Pd-Sb system (Fig. 6) were in the shape of needles. The composition of these single crystals is pure Pd.

The obtained single crystals of U-Ni-Sb system (Fig. 6) were in various shapes such as dendrites, cubes and plates. The obtained single crystals from both ampoules were analysed with the same composition of $U_3Ni_{11}Sb_6$.

The third series of $U_3T_3Sb_4$ materials were grown with In flux [7], because these materials are not so rich for Sb. Elements were mixed in stoichiometric ratio 0.33:0.33:0.4 (U:T:Sb) and added to In in ratio of 1:10. The ampoules were put in furnace with temperature profile in Figure 7.

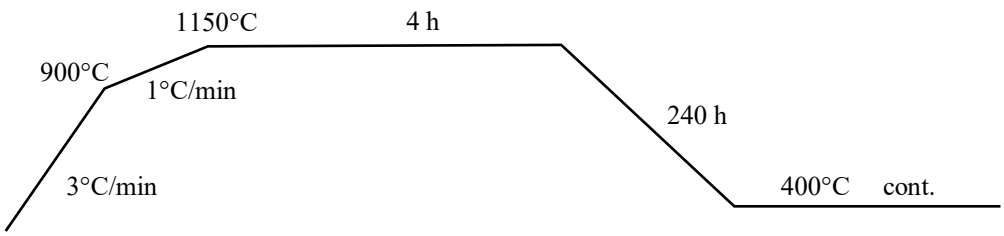

Figure 7: Temperature profile for $U_3T_3Sb_4$ single crystals grown from In flux.

The compositions of all obtained single crystals (Fig. 8) are the same T_7In_{12}. This might be because this binary phase is more stable than the desired $U_3T_3Sb_4$.

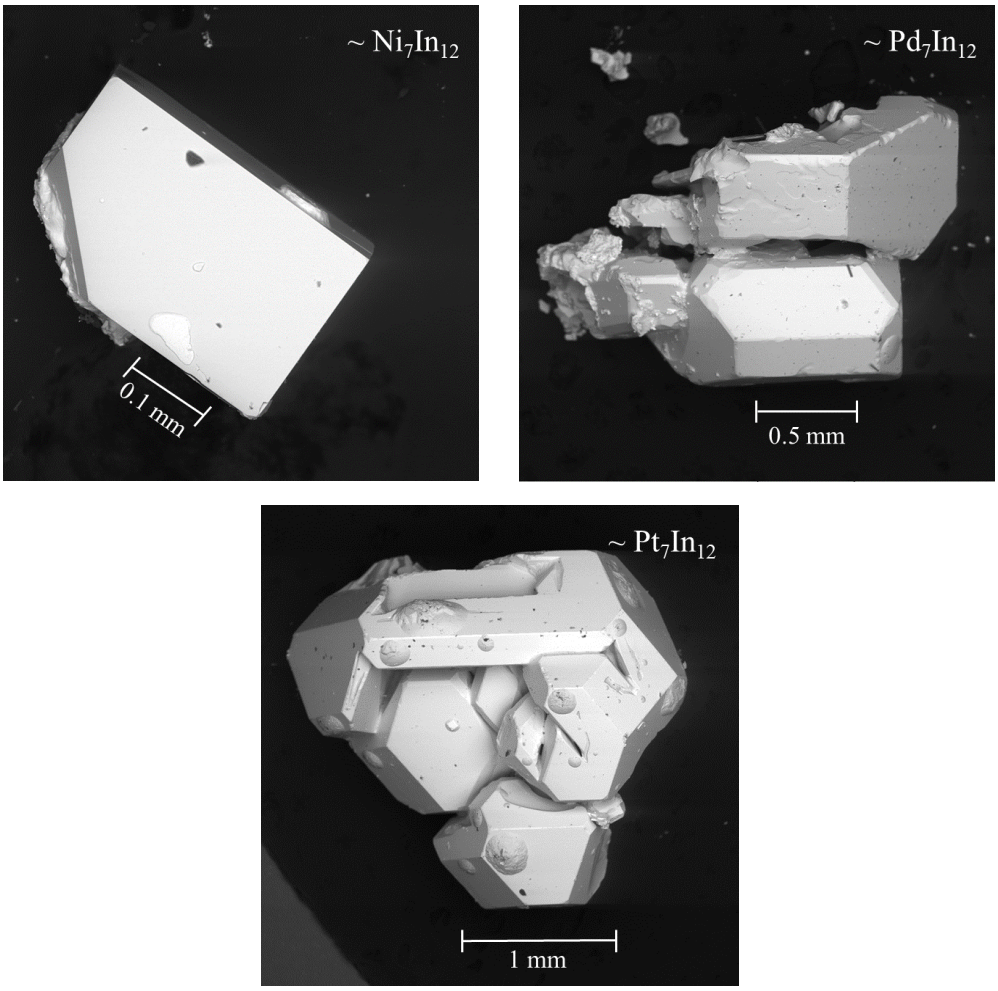

Figure 8: Single crystals of $U_3T_3Sb_4$ obtained from In flux.

2.1.3 $U_3T_3Bi_4$ series

The growth of the $U_3T_3X_4$ single crystals is a part of the bilateral Austrian – Czech research project on Topological Kondo Insulators based on Ce and U compounds. Since the Austrian group has managed to grow single crystals of $Ce_3Pt_3Bi_4$ and $Ce_3Pd_3Bi_4$, we decided to test $U_3T_3Bi_4$ with Bi instead of Sb.

For $U_3T_3Bi_4$ series, the constituent elements were mixed in the ratio 10:2:1 (Bi:T:U). The single crystals were grown from Bi flux in alumina crucible under vacuum in a quartz ampoule. The temperature profile and stoichiometric ratios were taken from the article about single crystal growth of $U_3Bi_4M_3$ (M = Ni or Rh) [8]. Figure 9 shows the temperature profile for the first series growth of $U_3T_3Bi_4$.

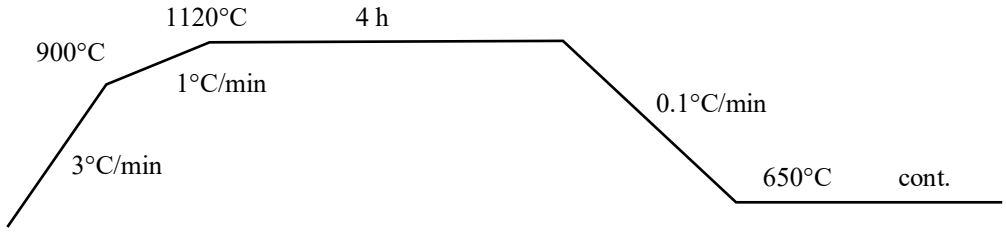

Figure 9: Temperature profile for first series of $U_3T_3Bi_4$ single crystals.

The only single crystals obtained from the bottom of crucible are shown in Figure 10. Since almost no single crystals were found in the top crucible the terminal temperature 650°C of the temperature profile was probably too high. I decided to repeat the experiment with lower terminal temperature 500°C. The altered temperature profile for second attempt is shown in Figure 11.

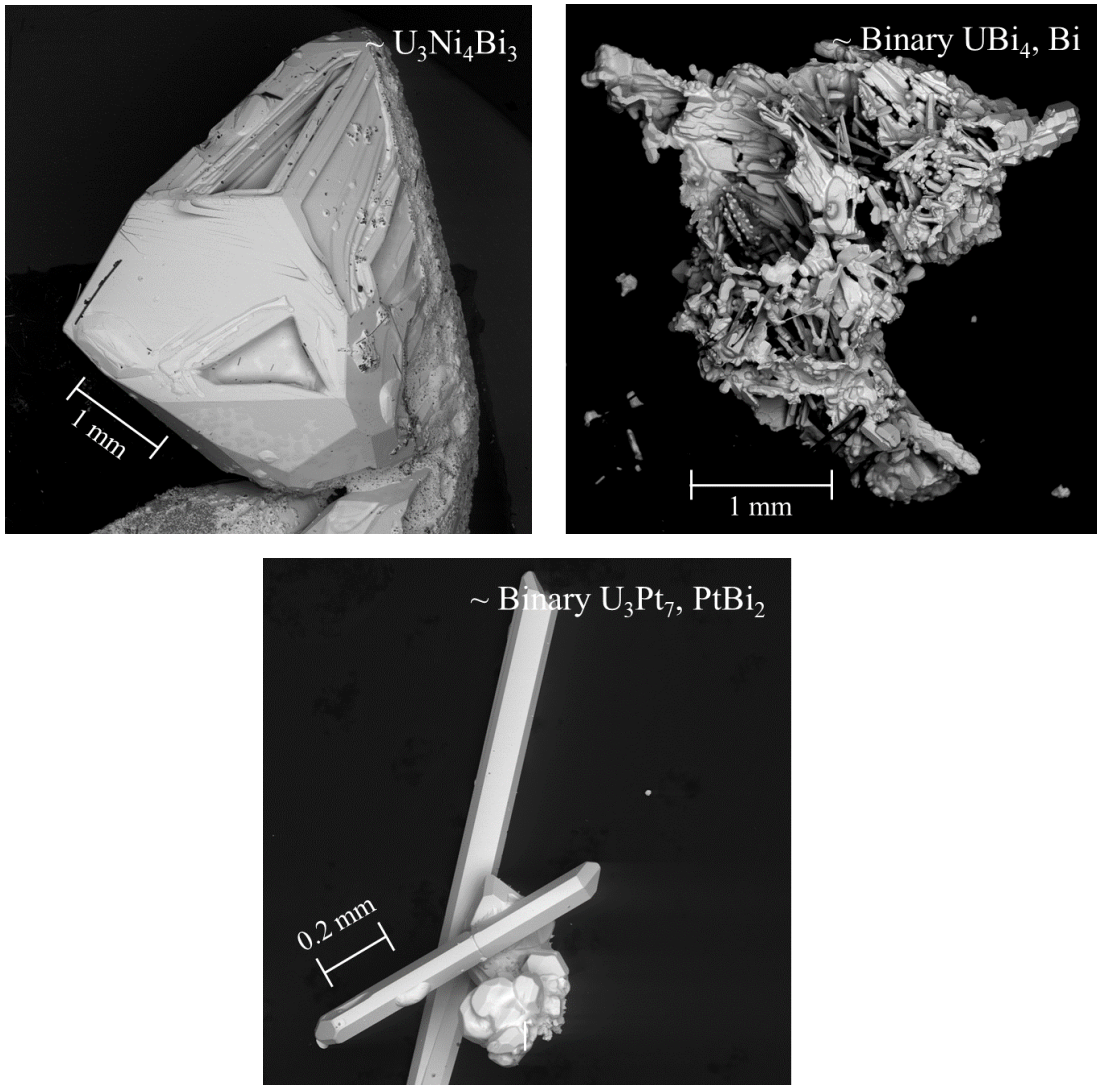

Figure 10: Single crystals obtained from the U-T-Bi system first series grown from Bi flux.

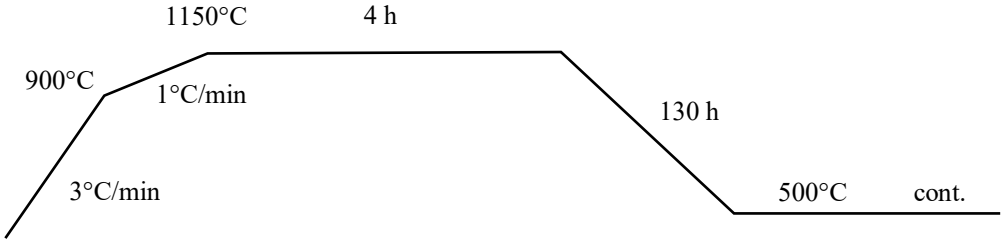

Figure 11: Temperature profile for second series of materials $U_3T_3Bi_4$.

The change of the final temperature solved our problem. Second series of $U_3T_3Bi_4$ materials was much more successful than the first one (Fig. 12).

No single crystals in U-Pd-Bi system were seen by naked eye. In Figure 12 you can see small black or white single crystals. The composition of the small black single crystals was found as $U_3Pd_4Bi_{13}$ and the composition of the white single crystals was pure uranium.

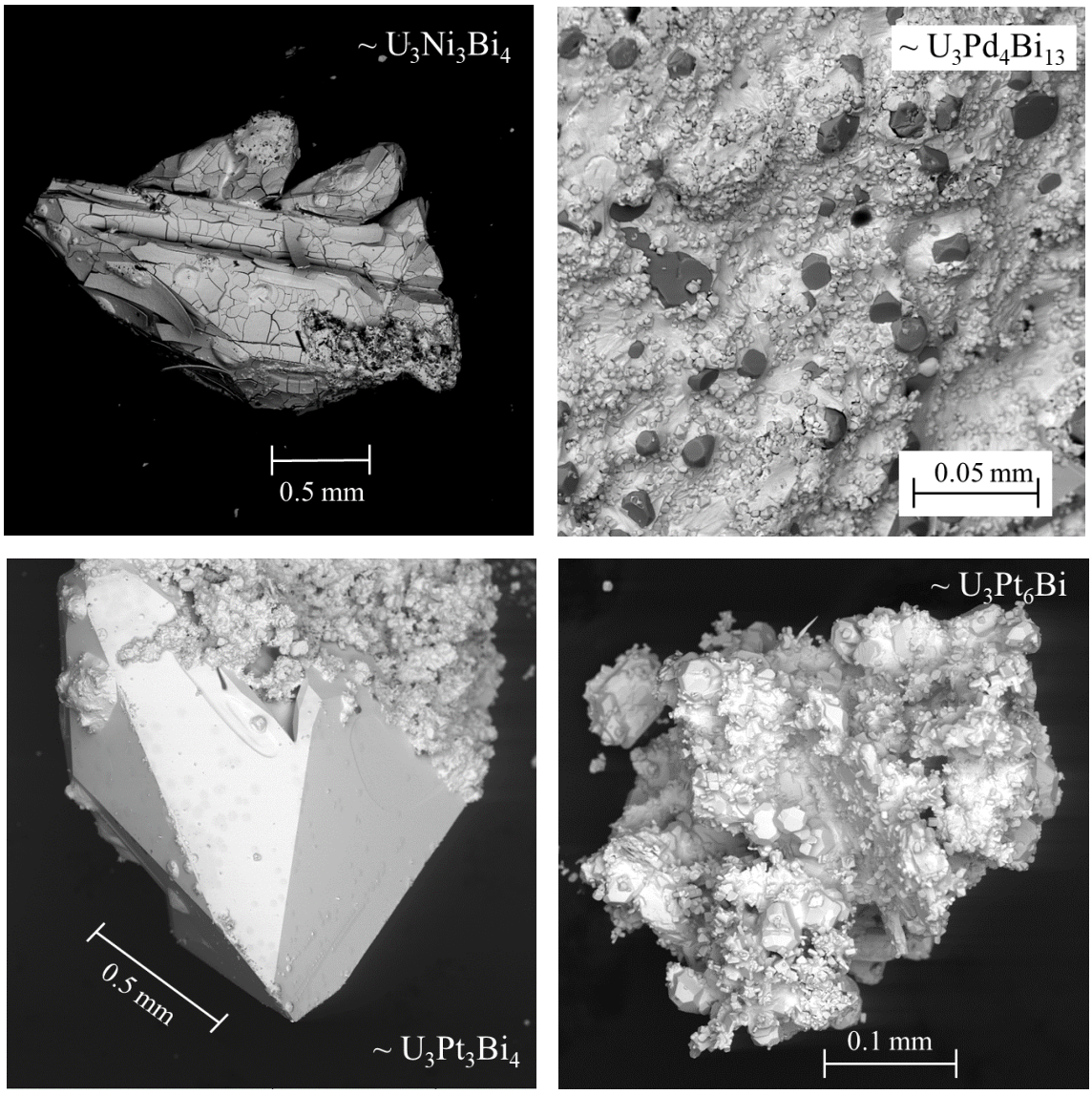

Figure 12: Single crystals obtained from the U-T-Bi system second series grown from Bi flux.

The composition of U-Ni-Bi system single crystals was confirmed as $U_3Ni_3Bi_4$. The surface cracking of the single crystal is probably caused by strong inner tension.

Chemical analysis of U-Pt-Bi system single crystals was rather complicated. In this system, two different single crystals of two different compositions were obtained (Fig. 12). The composition of the smaller single crystals on the big single crystals was found as U_3Pt_6Bi. The other single crystal was confirmed as $U_3Pt_3Bi_4$. So far this material has not been reported in single crystal form. The main problem is that the $U_3Pt_3Bi_4$ single crystals are very small 500 µm.

From the results, I assume that the growth of $U_3Pd_3Bi_4$ and $U_3Ni_3Bi_4$ depends strongly on the temperature profile during the growth. In future, I need to repeat this process again to understand which factors besides the temperature play a big role in the growth of $U_3T_3Bi_4$. The growth process also needs to be advanced in order to acknowledge the reproduction of the growth.

As mentioned before these materials are part of International Czech – Austrian project. I went to Technical University in Vienna to look how their process of growth and preparation of this class of materials based on Cerium under the supervision of Dr.rer.nat. Xinlin Yan. When growing $Ce_3T_3X_4$ they also try to dope Ce with La which is quite known substitution. In order to show me how they prepare the materials, we grew single crystals of $La_3Pd_3Bi_4$. Even though this compound does not have Ce the process is the same as for $Ce_3Pd_3Bi_4$. The purpose of this work travel was for me to gain some other perspective in growing of these materials and use it for single crystal growth of $U_3T_3X_4$ at our faculty. The Table 2 shows the used stoichiometric ratios.

Crystal – 40% (1 g)	
Elements	**Stoichiometric ratio**
La (4N)	3
Pd (3N5)	4.5
Bi (5N)	4

Flux – 60%	
Elements	**Stoichiometric ratio**
Bi (5N)	40%
Pb (5N)	60%

Table 2: The stoichiometric ratios of elements for crystals (left) and flux (right).

The flux is prepared from mixture of Bi and Pb. Presence of Pb in the flux raises the solubility of Bi and the ratio must be as close as it can get to 40% crystal and 60% flux because the system is very sensitive. First, we made alloy of La and Pd by arc-melting which we put in one crucible with flux of Bi and Pb. The scheme and picture of the ampoule after taking it out of furnace are in Figure 13.

The used temperature profile is showed in Figure 14. When we took out the crucible from the ampoule, we sorted out the single crystals suitable for powder diffraction and Laue diffraction to analyse if it is the single crystal and test the composition. Laue pattern with sharp spots confirmed single crystal form (Fig. 15). Powder diffraction pattern evaluated structure model confirmed $La_3Pd_3Bi_4$ composition (Fig. 16).

Figure 13: Scheme of prepared material (left) and ampoule after growth process (right).

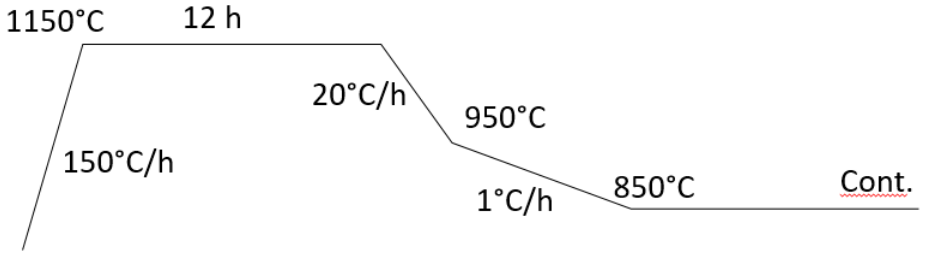

Figure 14: Temperature profile for growth of $La_3Pd_3Bi_4$.

Since this compound is known to crystallize in the cubic $Y_3Au_3Sb_4$ – type structure [8], the input cell parameter for the powder diffraction was $a = 10.1118\,\text{Å}$, to successfully evaluate the Laue pattern as well as the powder x-ray diffraction pattern.

The major differences in material preparation at the Technical University in Vienna were composition of the flux and different type of crucible. In future, we would like to try to grow $U_3T_3Bi_4$ using these preparation parameters.

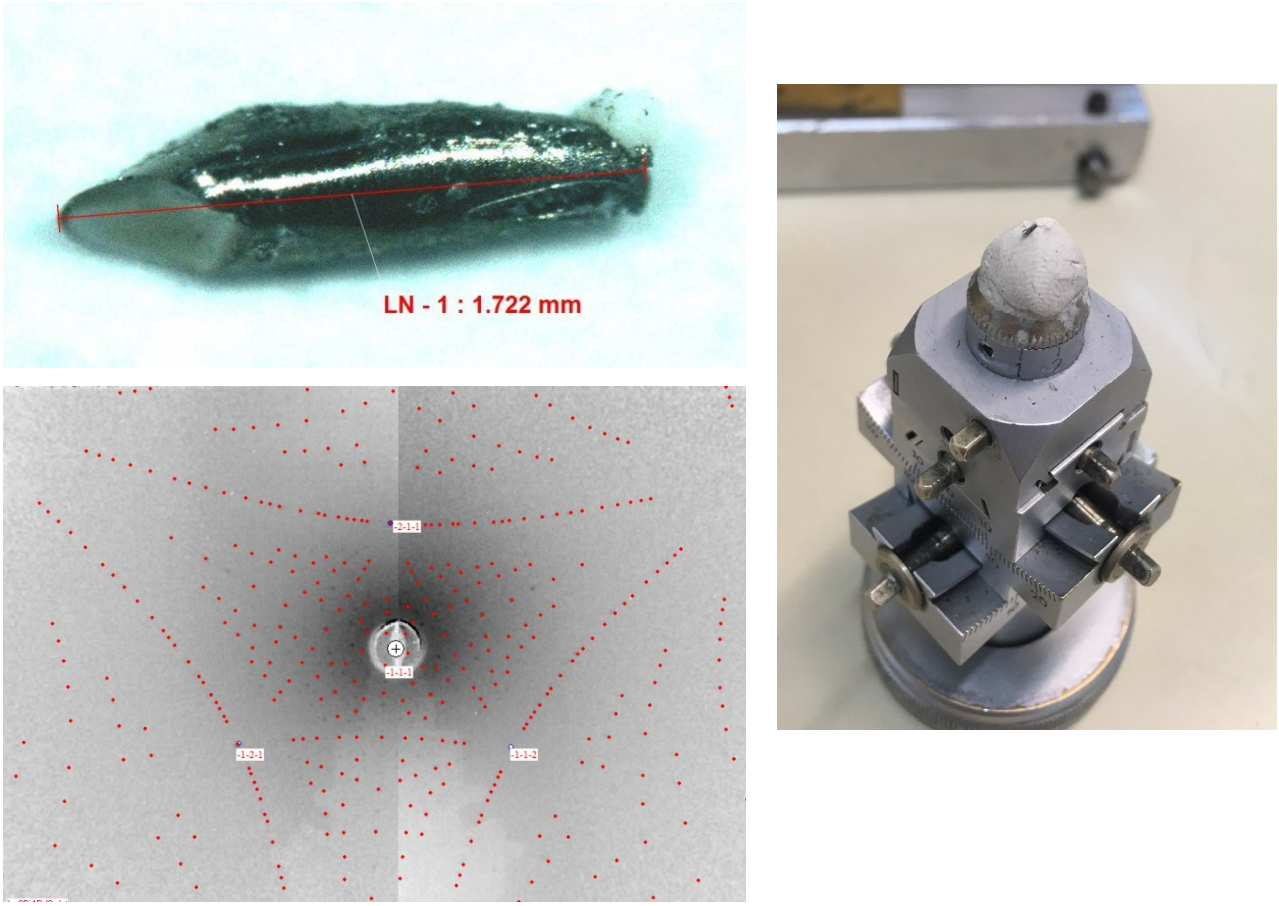

Figure 15: Single crystal of $La_3Pd_3Bi_4$ (top left), Laue diffractometer pattern (bottom left) and single crystal on goniometric head.

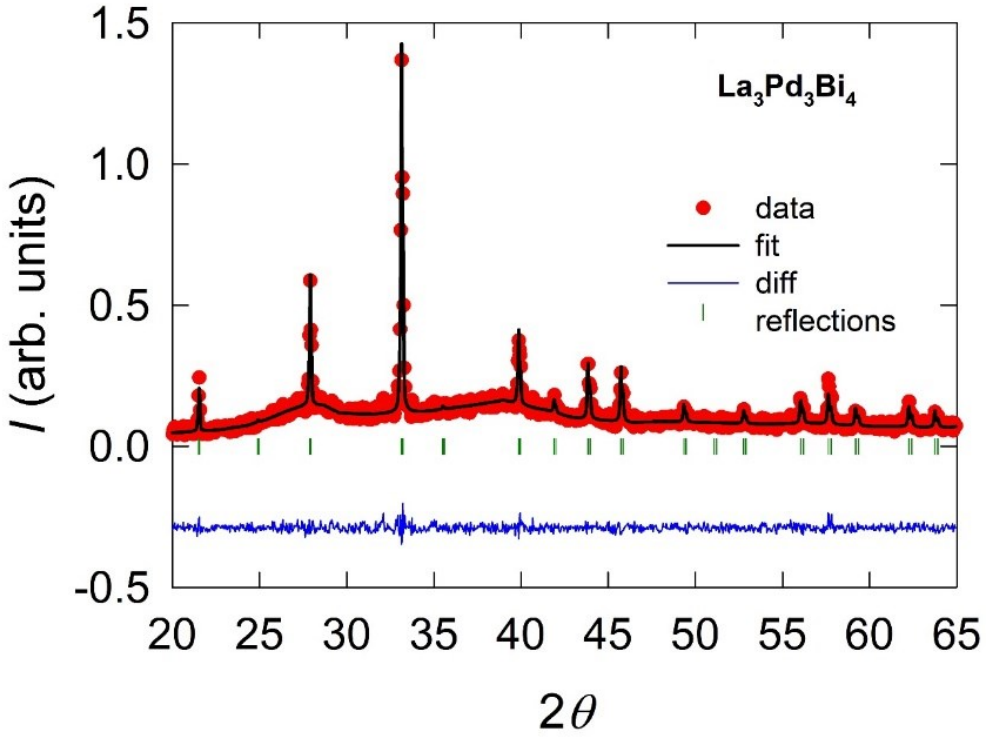

Figure 16: Powder diffraction pattern confirming the composition of $La_3Pd_3Bi_4$.

2.1.4 Ce_3Al_{11} series

The next type of material I tried to grow was $Ce_{3-x}La_xAl_{11}$ series. This compound has interesting magnetic properties. It orders ferromagnetically at T_C = 6.2 K which is followed by an antiferromagnetic transition at T_N = 3.4 K [9]. These compounds were grown from Al flux. I tried to dope the Ce with La with 5%, 10%, 15%, 20%, 30%, 50% and 100%. The temperature profile and ampoules taken out of centrifuge are in Fig. 17.

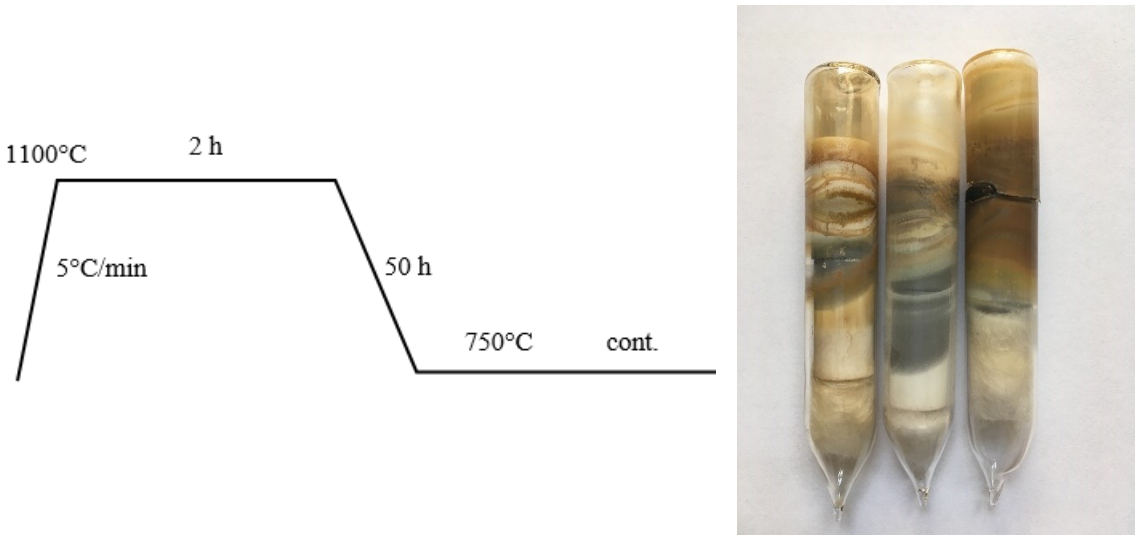

Figure 17: Temperature profile for growth of $Ce_{3-x}La_xAl_{11}$ (left) and ampoules after growth process (right).

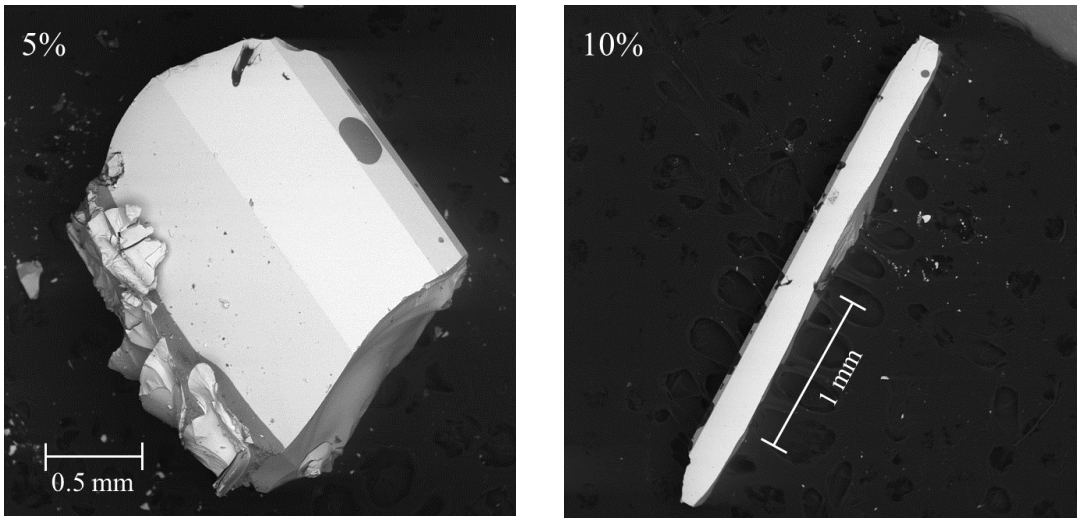

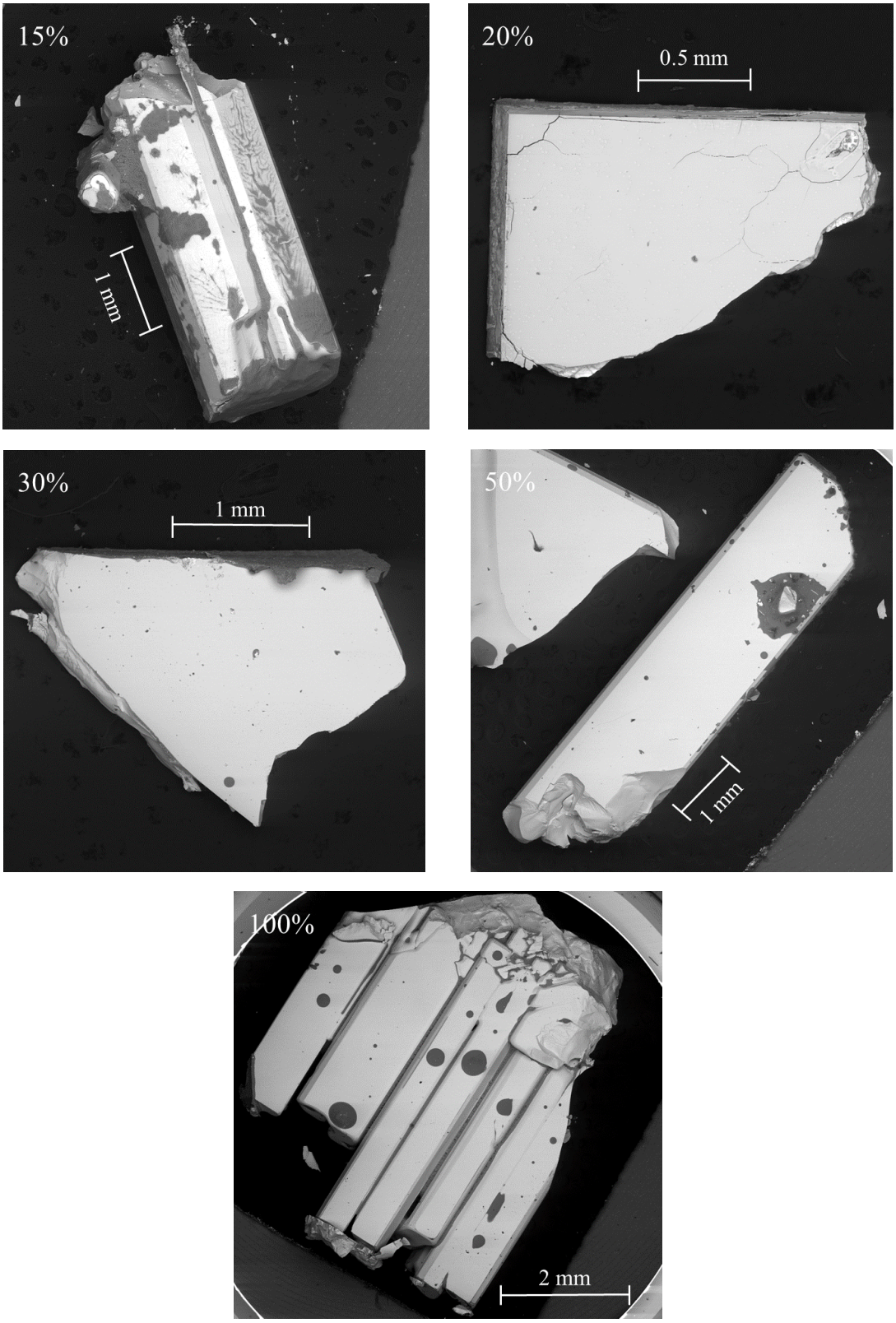

Figure 18: Single crystals of Ce-La-Al system.

The single crystals obtained were in a large scale (Fig. 18). These materials grew easily since they are basically binaries. The phase diagram for Ce and Al is well known which helps to determine the optimal preparation for the growth (Fig. 19). Laue diffraction was performed on the crystal of Ce_3Al_{11} and confirmed as single crystal (Fig. 20).

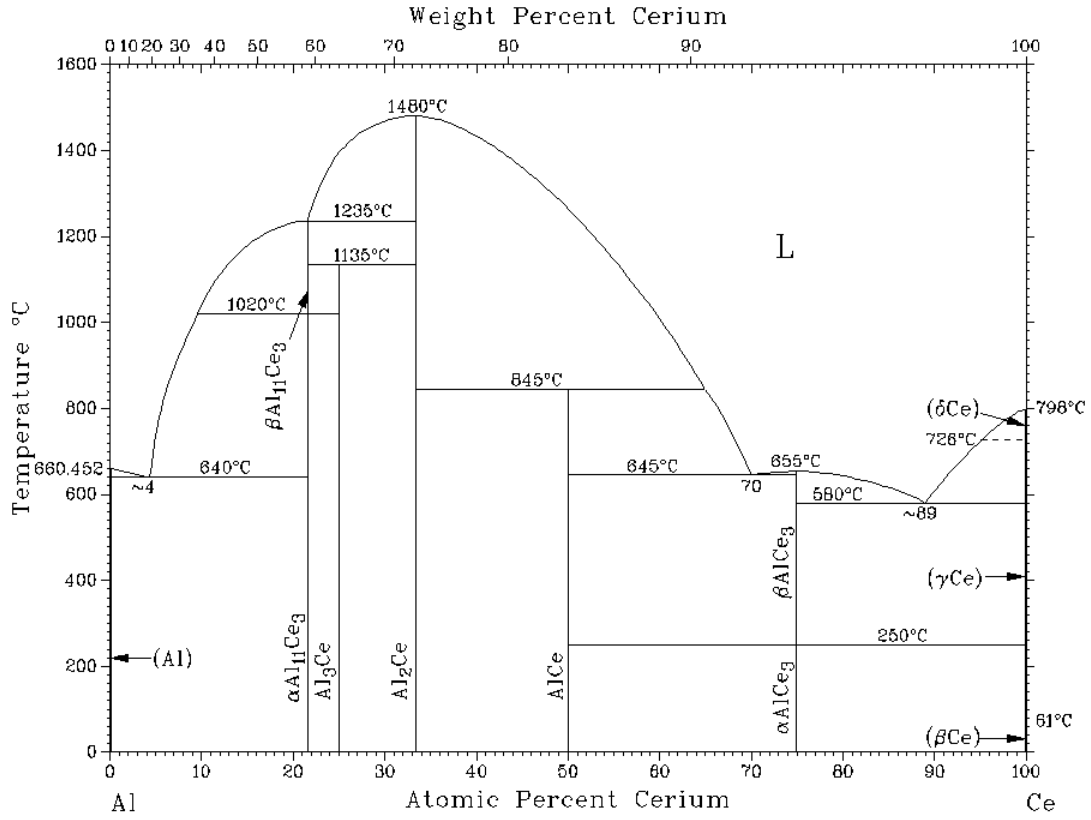

Figure 19: Phase diagram of Al – Ce in atomic percentage [4].

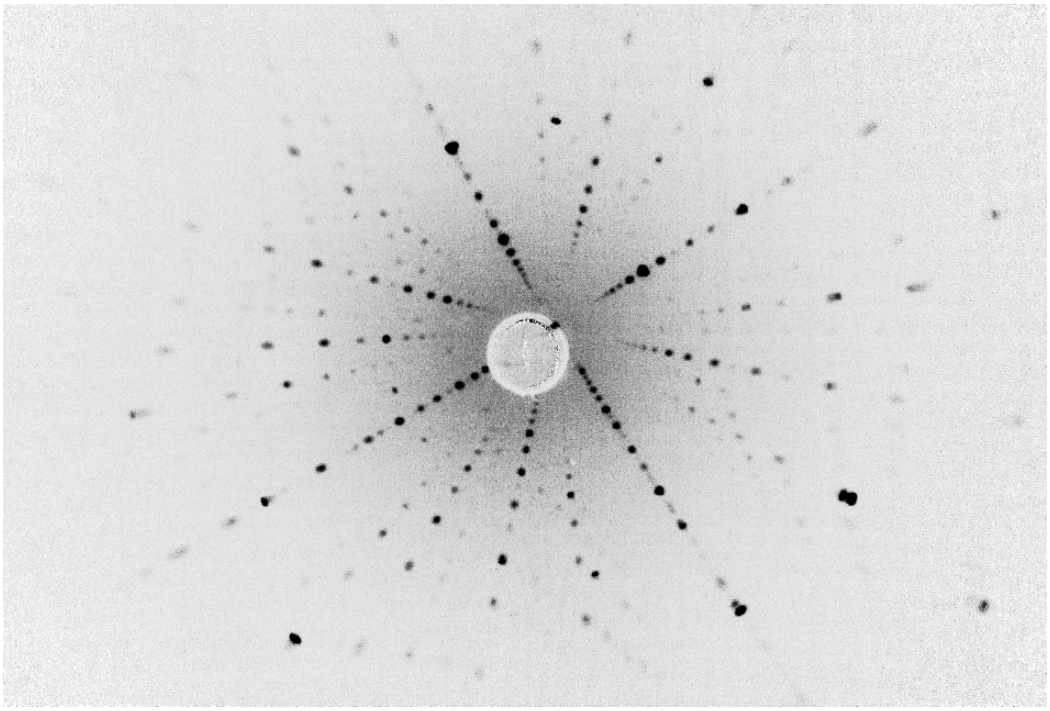

Figure 20: Laue diffraction pattern of Ce_3Al_{11} single crystal.

2.2 Bridgman method

2.2.1 Description of method

The next method used for the growth of single crystals was Bridgman method. In the first step, elements are mixed in stoichiometric ratio and melted in a mono-arc furnace to polycrystalline form. This polycrystalline sample in the form of button is powdered in an agate mortar. This boron nitride crucible with conically shaped bottom is fully filled by the powder. Then, the Boron Nitride crucible is scratched on the side in order to slide inside the Molybdenum capsule. The clean Mo capsule is closed by a welder under Ar atmosphere. The closed Mo capsule is inserted inside a water cooled evacuated quartz chamber to the centre of the induction coil and is heated up to desired temperature. The Boron Nitride crucible (BN crucible) is very soft and single crystal can be simply extracted by its peeling.

2.2.2 $U_3Pt_3Sb_4$ series

We grew single crystals of $U_3Pt_3Sb_4$ by Bridgman method. Elements were mixed in the stoichiometric ratio of 3:3:4.1 (U:Pt:Sb) and melted together in a mono-arc furnace. I documented the process of material preparation which is shown in Figure 21.

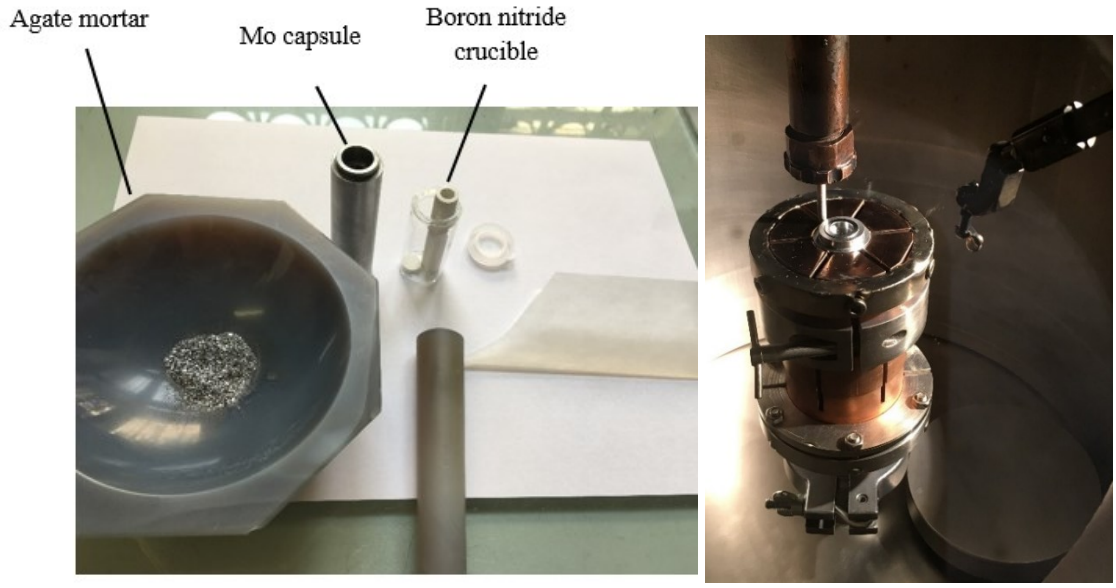

Figure 21: The material preparation (left) and sealing of Mo capsule (right).

The Mo capsule with prepared material inside was put in the induction furnace. The electrical power for the growth was set up to 2.8 kW with voltage of 330 V. The temperature reached 1400°C. However, the upper temperature was apparently not high enough to melt the powder. We repeated the process but with a higher temperature. I prepared the second material in the same way as the first one. I set up the electrical power for the growth to 4.2 kW with voltage of 430 V. The temperature went up to 1580°C. In Figure 22 it shows the running induction furnace and crucible after opening the Mo capsule.

Figure 22: Heating up of induction furnace (left) and the opened Mo capsule with BN crucible (right). It is possible to see the scratch on the side of the BN crucible.

The single crystal in a shape of the ingot was obtained (Fig. 23) and the Laue diffraction (Fig. 24) was performed on this single crystal. The diffraction confirmed single crystal based material. The composition of these single crystals was found as U_6Pt_3Sb. The measured composition is interesting because of its low concentration of Sb. This might be caused due to extremely high temperature for Sb. Antimony has melting temperature around 600°C. It is possible that the antimony vaporized or started to react with the BN crucible or Mo capsule.

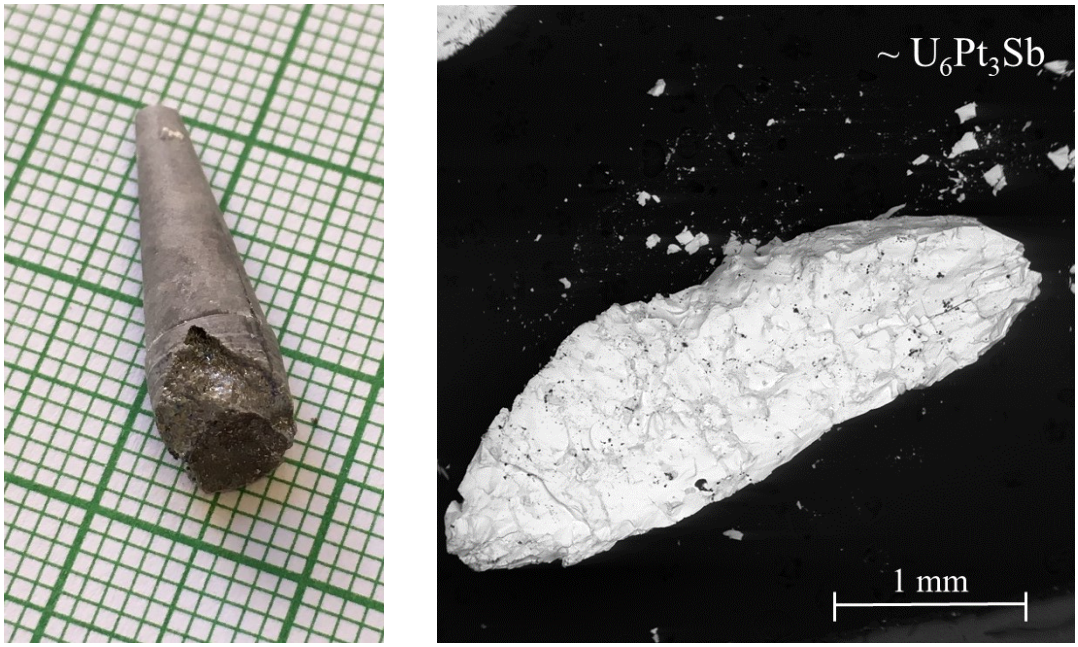

Figure 23: Single crystals of U-Pt-Sb system.

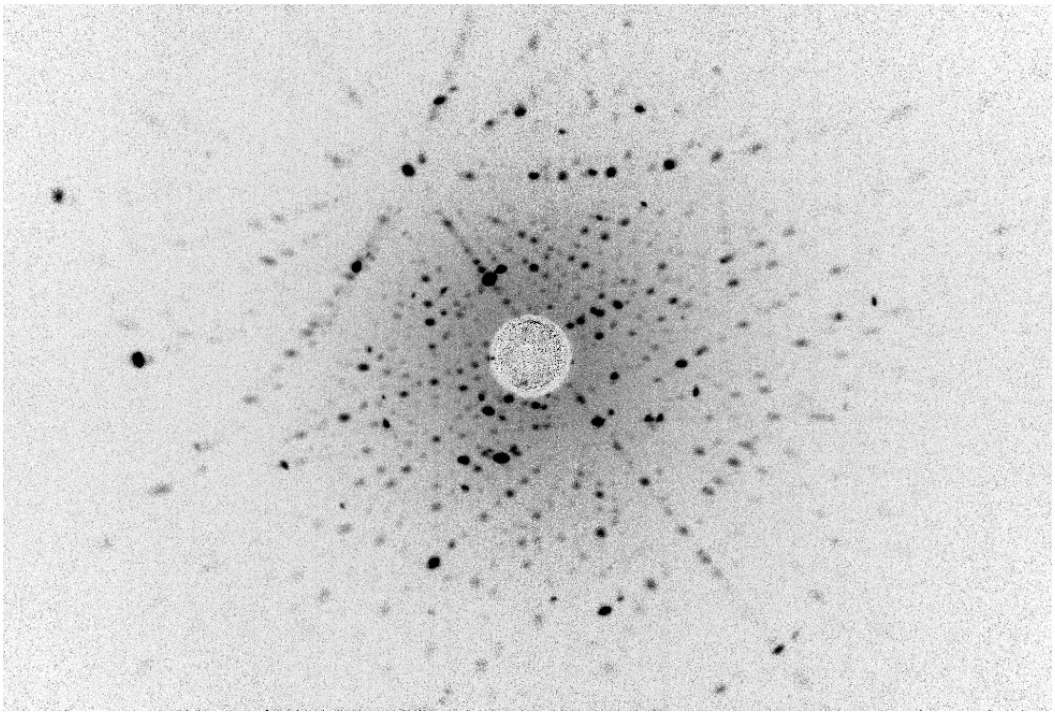

Figure 24: Laue diffraction image of single crystal of $U_3Pt_3Sb_4$.

2.3 Czochralski method

2.3.1 Description of method

Another single crystal growth method was the Czochralski method. The elements are put into the mono-arc furnace and melted under argon protective atmosphere. The obtained polycrystalline precursor is placed on copper crucible in a tri-arc furnace and kept by fine regulation above the melting point of the alloy. If we have polycrystalline or heterogeneous material as a seed rod, it is necessary to create a narrow neck to select one grain, which will propagate in the further grown ingot.

2.3.2 U_2Ru_2Sn

I have grown semimetallic U_2Ru_2Sn by Czochralski method. Pure elements were mixed in stoichiometric ratio 2:2:1.03 (U:Ru:Sn). An extra 3% of Sn was added because of its higher evaporation. Stabilization of the narrow neck was difficult. The biggest problem of this growth was fluctuation of current during growth (Fig. 25). Since the compound contains Sn it started to react with the Cu crucible and acted as glue. This led to sudden solidification of the melt. Since the crystal broke at the end of growth process, it was not so easy to do a composition analysis and Laue diffraction.

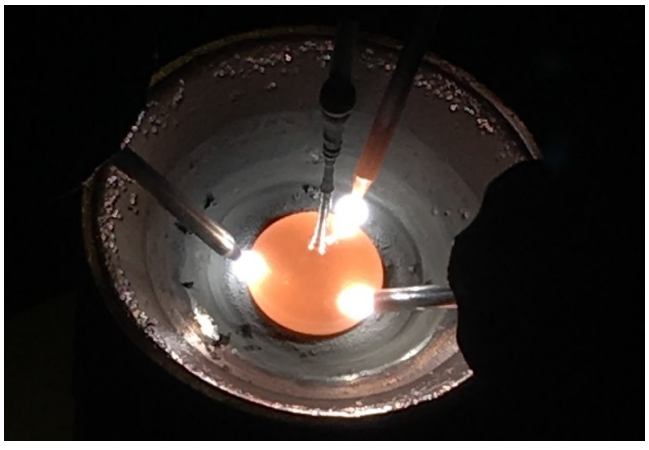

Figure 25: Single crystal of U_2Ru_2Sn grown by Czochralski method.

2.3.3 $UCo_{0.95}Ir_{0.05}Ge$

$UCo_{0.95}Ir_{0.05}Ge$ is UCoGe doped by Ir. UCoGe is known as a ferromagnetic superconductor [10]. Procedure of the polycrystalline precursor and single crystal is identical with U_2Ru_2Sn. Elements were mixed in stoichiometric ratio 1:0.95:0.05:1.03 (U:Co:Ir:Ge) and melted in the mono-arc furnace under argon protective atmosphere. An extra 3% of Ge was added due to its higher evaporation [11]. The electric current during the connecting the seed rod with the melt was 15 A and slowly increasing by 0.3 A steps. Velocity of pulling was 10 mm/h under 19 A. During narrowing the velocity was lowered to 6 mm/h and the electric current was slowly decreasing by 0.2 A steps. Laue diffraction was performed on the grown ingot and confirmed single crystal (Fig. 26) by recorded symmetrically ordered sharp reflections. The chemical composition corresponded with the nominal one.

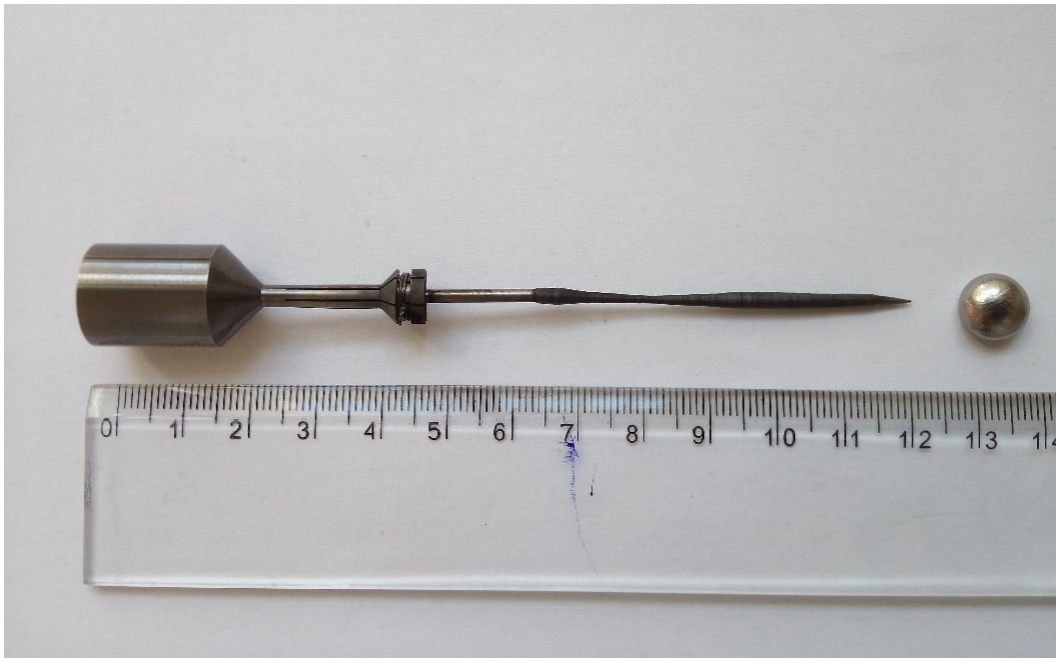

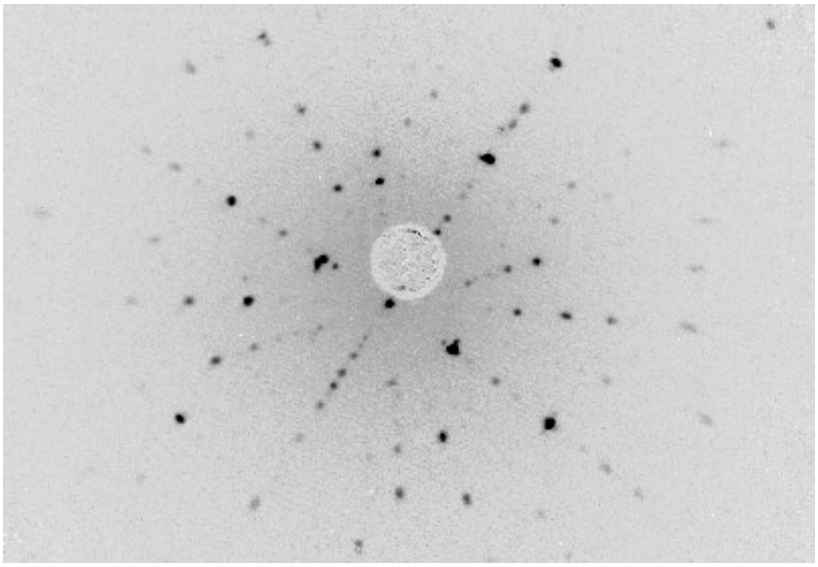

Figure 26: Laue pattern (bottom) of the single crystal $UCo_{0.95}Ir_{0.05}Ge$ (top).

2.4 Floating Zone method

2.4.1 Description of method

All experiments by the floating zone method were carried out in laser and mirror furnaces made in Crystal Systems Corporation Company in Kobuchisawa, Japan (Fig. 27). The mirror furnace can work with four possible atmospheres for growth: Ar, N_2, O_2 and air. Since this furnace also has high vacuum option, it is suitable even for growth of metallic materials.

There are two ways how to prepare polycrystalline precursors for single crystal growth by floating zone method in optical and laser furnace. Metallic materials are prepared by casting in special bar-shaped cusp in the mono-arc furnace under the argon atmosphere into the polycrystalline rod. Oxides are usually in the form of a powder. If the material consists of multiple oxides it is necessary to prepare a homogenous mixture powder. This powder mixture is put into a rubber tube. After filling the rubber tube, the powder is compressed by pressure of 2 tons/cm^2 in a hydrostatic cell. A small hole is

drilled through the rod for a hook in order to place the precursor in a furnace. The precursor rod is sintered in a chamber furnace at a temperature of 20-30% below melting point for one day. The precursor is placed in the optical furnace inside transparent quartz chamber in which different atmospheres for single crystal growth are available in the pressure range 10^{-6} mbar - 10 bar.

Figure 27: Optical furnace with 4 ellipsoidal mirrors (top left), prototype of a high pressure laser furnace with 3 lasers (bottom left) and the brick calibration cylinder (right).

2.4.2 Sapphire-base materials

First single crystals grown by floating zone method were sapphire-based materials. Pure colourless sapphire consists only of Al_2O_3. The first was synthetic ruby (Fig. 28). Ruby is a red modification of sapphire which is caused by 0.5 % trace of the Cr_2O_3. Prepared precursor was put in the optical mirror furnace under air. The temperature during growth went approximately up to 2100°C. This is almost the upper limit of the furnace which power was set to 95-100 % (4 kW). The cracks occurred during the growth. This was probably caused due to fast pulling of the precursor through the molten zone by 10 mm/h.

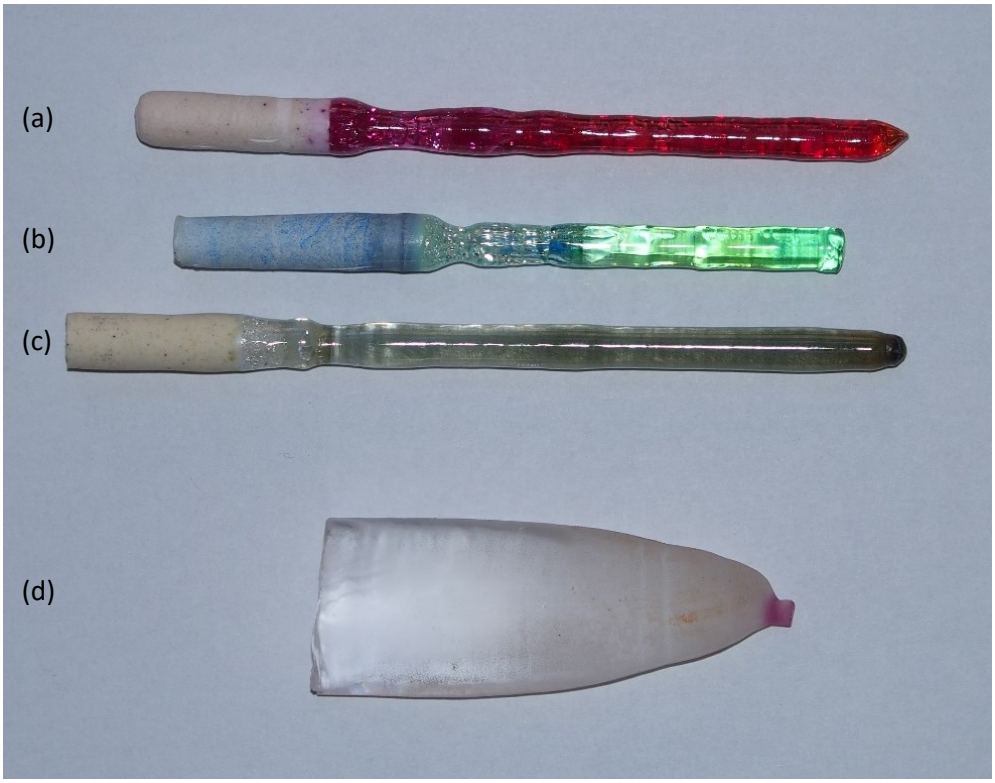

Figure 28: (a) single crystal of Ruby doped with Cr_2O_3, (b) single crystal of blue sapphire doped with Co_2O_3, (c) single crystal of sapphire doped with Fe_2O_3 and (d) example of colourless single crystal of pure sapphire grown by Verneuil method.

Other two precursors were doped with 5% of Co_2O_3 and 0.5% of Fe_2O_3 (Fig. 28). The single crystal with Co_2O_3 is the known to be blue sapphire; however, we have received a green modification likely due to change of the valence state of Co ions on air. The growth condition was identical with the red ruby; interestingly, we have not detected any cracks inside the single crystal. The sapphire modification substituted by Fe_2O_3 was grown in the laser furnace. We needed 60% (600 W) of power due to a very well-focused laser beam in contrast with a much wider hot zone in the mirror furnace, in which the majority of the heat is only energy loss, due to improper focussing and scattering of the light. The obtained green single crystal with its blue precursor as well as the filled rubber capsule is shown in Figure 29.

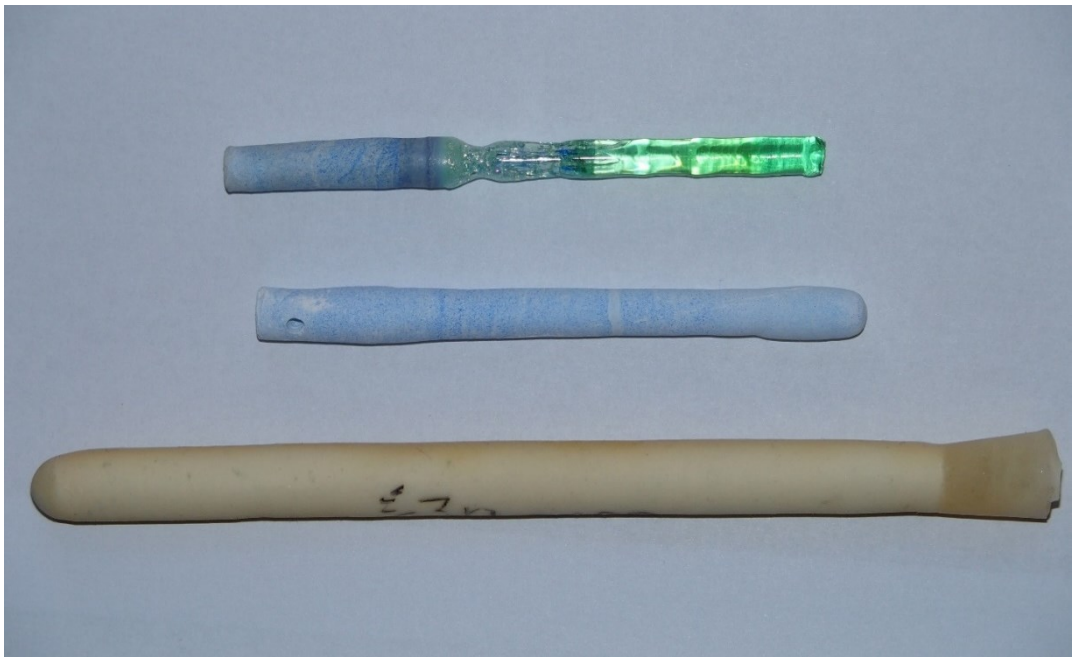

Figure 29: Single crystal of sapphire doped with Co_2O_3 (top), sintered rod precursor with drilled hole (middle) and the rubber tube filled by powder (bottom).

2.4.3 UNiSn

The next material I grew by floating zone method in mirror furnace was UNiSn. This material had been studied before because of its antifferromagnetic and possible semimetallic properties [12]. The pure elements were mixed in stoichiometric ratio of 1:1:1 and melted in mono-arc furnace to polycrystalline precursor which were casted to the form of rod. During the growth process we reached 40% of the furnace power. No problems occurred during the growth process. In Figure 30 is shown hot zone with the melt trapped between upper polycrystalline sample and bottom growing ingot. The pulling speed was very slow, only 1mm/h. Laue diffraction and composition analysis was performed on prepared ingot. The Laue pattern (Fig. 30) confirmed high quality of single crystal by symmetrically arranged sharp reflections.

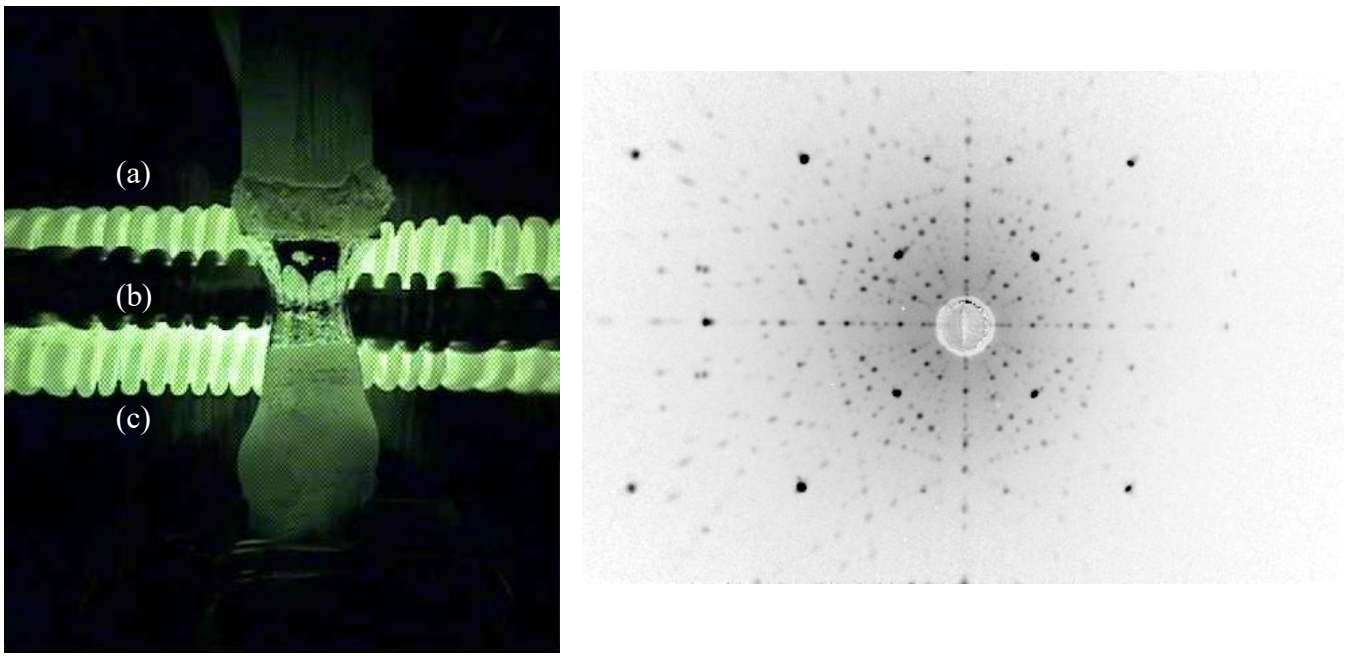

Figure 30: Growing single crystal of UNiSn in optical furnace (left): (a) polycrystalline precursor rod, (b) molten zone, (c) single crystal and Laue diffraction pattern performed on a single crystal (right).

2.5 Chemical vapour transport method

2.5.1 Description of method

During this method, elements forming the expected materials are put on a bottom of a quartz tube. In glass sealing station the ampoule is sealed under vacuum. The ampoule is placed in the gradient furnace horizontally. After the growth process the ampoule is simply taken out of the furnace and opened up by cracking the walls of the ampoule.

2.5.2 VI_3 series

VI_3 compound is known as van der Waals ferromagnet [13]. Three series of this material were prepared with the same stoichiometric ratio 2:3 ($V:I_2$). An extra 3% of I_2 was added due to its high evaporation. The three processes were performed with different temperature profiles. The temperature profile for the first process is shown in Figure 31.

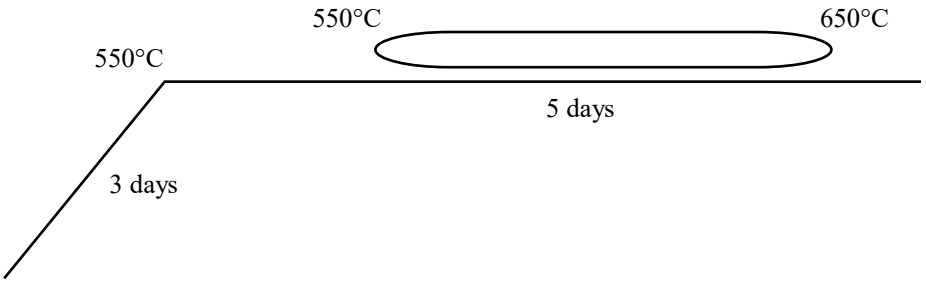

Figure 31: Temperature profile for first series of material VI_3.

VI_3 crystalizes in hexagonal structure and under optical microscope was possible to see small single crystals in hexagonal shape (Fig. 32). The other two attempts were not so successful due to oxidation of the elements during preparation. It seems like the

purity of elements in the sense of oxidation of metallic component is crucially important in order to grow single crystals of VI_3.

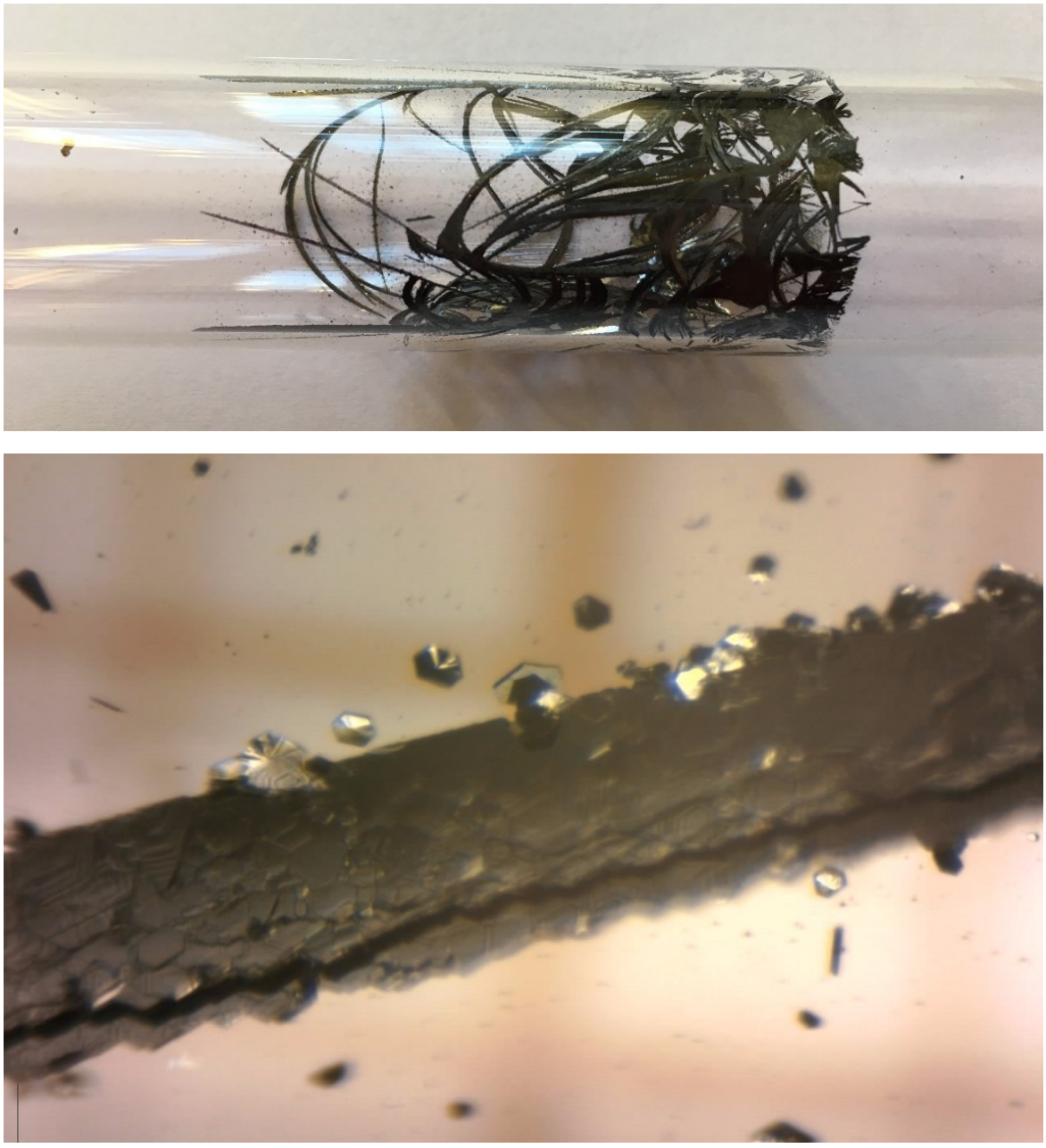

Figure 32: Single crystal in ampoule (top) and single crystals with hexagonal shape under optical microscope.

Conclusions

The ternary materials $U_3T_3X_4$ were tested to grow by flux for T = Ni, Pd and Pt are transitional metals and X = Sb or Bi. The growth process for Sb series was not possible to optimize. I finally obtained single crystals of $U_3Ni_3Bi_4$ and $U_3Pd_3Bi_4$, where single crystal of $U_3Pd_3Bi_4$ was not mentioned in literature before. Critical parameters were an unknown phase diagram and, also, low concentration of the solvent in the target compounds. On the other hand, single crystals of the binary Ce_3Al_{11} system doped with La were produced in the large scale. In this case, the phase diagram of this binary system is well-known.

I decided to test the growth of $U_3Pt_3Sb_4$ material by Bridgman method instead of flux since we obtained mainly binaries USb_2 and $PtSb_2$. Finally, I grew single crystal but with a slightly different composition of U_6Pt_3Sb. In second attempt the temperature might have been too high temperature and initialized a reaction of the Mo crucible with antimony gas.

The Czochralski method was used to grow U_2Ru_2Sn and $UCo_{0.95}Ir_{0.05}Ge$ single crystals. Both compounds are congruently melting. The growth of $UCo_{0.95}Ir_{0.05}Ge$ was very stable and a nice cylindrical single crystal was obtained. U_2Ru_2Sn was much more complicated due to instability caused by evaporation of the tin from the melt, which reacted with copper crucible and mediated thermal contact. Therefore, materials with strong evaporation are not suitable for Czochralski method.

The sapphire-based materials and UNiSn were grown by Floating Zone method in mirror and laser optical furnaces. I obtained single crystals of various sapphire materials. The floating zone method is suitable for growth of sapphire materials and oxide materials. However, the halogen furnace is strongly limited by its power. In the case of laser furnace maximum power is four times lower but upper attainable temperature over 2600°C. The laser furnace is more suitable for the materials with the higher melting temperature.

The last method used for the growth of VI_3 was chemical vapour transport method. The products from this method – composition and size are strongly dependent on temperature gradient, purity of input elements and amount of the transport medium.

References

[1] K. Gibson, The role of single crystals in creating new materials, Phys.org. (2017). https://phys.org/news/2017-03-role-crystals-materials.html (accessed April 10, 2020).

[2] MGML.eu. (2020). https://mgml.eu/ (accessed May 23, 2020).

[3] T. Takabatake, et al., Semiconducting and heavy-fermion behavior in new class of materials of $U_3T_3X_4$, Physica B: Condensed Matter. 165-166 (1990) 437–438. doi:10.1016/s0921-4526(90)81068-y.

[4] Navigation, ASM Alloy Phase Diagram Database™ - ASM International. (n.d.). https://www.asminternational.org/materials-resources/online-databases/-/journal_content/56/10192/15469013/DATABASE (accessed May 28, 2020).

[5] J. Qi, et al., Measurement of Two Low-Temperature Energy Gaps in the Electronic Structure of Antiferromagnetic USb_2 Using Ultrafast Optical Spectroscopy, Physical Review Letters. 111 (2013). doi:10.1103/physrevlett.111.057402.

[6] A. Dargys, J. Kundrotas, Electrical properties of narrow gap semiconductor $PtSb_2$, Journal of Physics and Chemistry of Solids. 44 (1983) 261–267. doi:10.1016/0022-3697(83)90061-6.

[7] V.H. Tran, et al., Coexistence of antiferromagnetic and spin-glass behaviour in $U_3Rh_3Sb_4$, Journal of Physics: Condensed Matter. 17 (2005) 3597–3609. doi:10.1088/0953-8984/17/23/012.

[8] T. Klimczuk, et al., Physical properties of the uranium ternary compounds $U_3Bi_4M_3$ (M=Ni,Rh), Physical Review B. 77 (2008). doi:10.1103/physrevb.77.245111.

[9] A. Bendová, et al., Renewed Single Crystal Study of Ce_3Al_{11}, Proceedings of the International Conference on Strongly Correlated Electron Systems (SCES2019). (2020). doi:10.7566/jpscp.30.011108.

[10] N.T. Huy, et al., Superconductivity on the Border of Weak Itinerant Ferromagnetism in UCoGe, Physical Review Letters. 99 (2007). doi:10.1103/physrevlett.99.067006.

[11] J. Pospíšil, et al., Effect of Pressure on Magnetism of UIrGe, Journal of the Physical Society of Japan. 86 (2017) 044709. doi:10.7566/jpsj.86.044709.

[12] M. Yethiraj, et al., Magnetic and crystallographic properties of UNiSn, Journal of Magnetism and Magnetic Materials. 79 (1989) 355–357. doi:10.1016/0304-8853(89)90191-1.

[13] P. Doležal, et al., Crystal structures and phase transitions of the van der Waals ferromagnet VI3, Physical Review Materials. 3 (2019). doi:10.1103/physrevmaterials.3.121401.